

## ***In situ* silicon oxide based intermediate reflector for thin-film silicon micromorph solar cells**

P. Buehlmann,<sup>a)</sup> J. Bailat, D. Dominé, A. Billet, F. Meillaud, A. Feltrin, and C. Ballif

*Institute of Microtechnology (IMT), University of Neuchâtel, Rue A.-L. Breguet 2, CH-2000 Neuchâtel, Switzerland*

We show that SiO-based intermediate reflectors (SOIRs) can be fabricated in the same reactor and with the same process gases as used for thin-film silicon solar cells. By varying input gas ratios, SOIR layers with a wide range of optical and electrical properties are obtained. The influence of the SOIR thickness in the micromorph cell is studied and current gain and losses are discussed. Initial micromorph cell efficiency of 12.2% ( $V_{oc}=1.40$  V, fill factor=71.9%, and  $J_{sc}=12.1$  mA/cm<sup>2</sup>) is achieved with top cell, SOIR, and bottom cell thicknesses of 270, 95, and 1800 nm, respectively.

A micromorph tandem solar cell consists of a high-gap amorphous (*a*-Si:H) top cell and a low-gap microcrystalline silicon ( $\mu$ c-Si:H) bottom cell stacked on top of each other. The thickness of the *a*-Si:H cell has to be kept reasonably thin to minimize the impact of light-induced degradation,<sup>1</sup> and its current, therefore, generally limits the current of the tandem device. To overcome this issue, an intermediate reflecting layer (IRL) can be introduced between the two cells to increase the current of the top cell.<sup>2</sup> For an intermediate layer to act as a reflector, its refractive index  $n$  must be lower (typically  $n_{IRL} \approx 2$ ) than that of silicon ( $n_{Si}=3.8$  at 600 nm) such as to produce a refractive index step that causes the reflection of light at the material interface. The layer which serves as IRL is required to be sufficiently conductive to avoid blocking current and as transparent as possible to minimize the current losses due to absorption of light outside the active layers. In the first attempts to realize this intermediate reflector, zinc oxide (ZnO) has been used.<sup>2-4</sup> In a recent study, the top-cell current could be increased by 2.8 mA/cm<sup>2</sup>, using a 110-nm-thick ZnO IRL with a 180-nm-thick top cell.<sup>3</sup> When considering industrialization, there are, however, two main drawbacks of ZnO-based IRL: the need for an additional *ex situ* deposition step and an additional laser scribe for monolithic series interconnection to avoid lateral shunting of solar module segments.<sup>5</sup> Another group reported *in situ* fabrication of a different IRL but without specifying the material used.<sup>6</sup> In this paper, we propose the preparation of an IRL based on a “doped silicon oxide” material fabricated by plasma enhanced chemical vapor deposition (PECVD) in the same reactor as the solar cells. We demonstrate that it is possible to produce such a SiO-based intermediate reflector (SOIR), with a refractive index close to 2 and electrical properties suitable for incorporation into micromorph devices.

The SiO-based layers are deposited by very-high frequency PECVD at 110 MHz, 200 °C, and with a power density of 0.01–0.1 W/cm<sup>2</sup>. Optical and electrical characterizations are performed on ~100-nm-thick layers deposited on glass. Optical reflectance and transmittance are measured with a Perkin-Elmer photospectrometer, type lambda 900, within a spectral range from 320 to 2000 nm. The refractive

index  $n$  and the absorption coefficient  $\alpha$  are estimated by fitting the transmittance and reflectance spectra with dedicated software.<sup>7</sup> For electrical characterization, aluminum contacts are evaporated onto the samples and the in-plane dark conductivity is measured as a function of temperature after an annealing in vacuum for 1 h 30 min, at 180 °C. The silicon crystalline fraction is measured by Raman spectroscopy with a laser at a wavelength of 514 nm and evaluated as described by Droz.<sup>8</sup> The *p-i-n* micromorph cells are either deposited in a KAI-S deposition reactor or in a smaller laboratory system by PECVD on a rough front ZnO layer, deposited by low-pressure chemical vapor deposition.<sup>9</sup> The intrinsic layer thicknesses are between 250 and 270 nm for the *a*-Si:H and 1800 nm for the  $\mu$ c-Si:H cell. The SiO-based layers incorporated in the micromorph solar cell are deposited with gas flow ratios of  $PH_3/SiH_4=0.024$  and  $CO_2/SiH_4=2.7$ . *n*-type doping by phosphorous is chosen since *n*-type doping is usually more efficient than *p*-type doping. The cells are patterned to an area of 1.2 cm<sup>2</sup>. The absorbance  $A$  is calculated from the reflectance  $R$  by  $A=1-R$ , since the transmittance is zero due to the opaque, nonconducting back reflector used for the solar cells. The short-circuit current density ( $J_{sc}$ ) of the solar cells is calculated from the measurement of the external quantum efficiency (EQE) curve, by integrating, over the wavelength range from 350 to 1100 nm, the product of EQE times the incoming photon flux of the AM1.5g solar spectrum. The current density–voltage curves are measured under a dual lamp WACOM solar simulator in standard test conditions (25 °C, AM1.5g spectrum, and 1000 W/m<sup>2</sup>).

Figure 1 shows the refractive index  $n$  and the absorption coefficient  $\alpha$  versus the  $CO_2/SiH_4$  gas flow ratio at a wavelength of 600 nm.  $n$  decreases from 3 to 1.95 as the  $CO_2/SiH_4$  gas flow ratio increases from 0.5 to 6. For the same range,  $\alpha$  decreases from  $1 \times 10^4$  down to  $2 \times 10^3$  cm<sup>-1</sup>, which, for a 100-nm-thick layer, corresponds to a decrease in absorbance from 10% to 2%. For a typical SiO-based layer as incorporated in the micromorph cells,  $n$  is below 2.2 for the wavelengths above 500 nm, which corresponds to the part of the solar spectrum that reaches the IRL.

For a fixed  $CO_2/SiH_4$  gas flow ratio of 1.6, the conductivity of the deposited layers is increased by ten orders of magnitude by increasing the  $PH_3/SiH_4$  ratio from 2‰ to

<sup>a)</sup>Electronic mail: peter.buehlmann@unine.ch

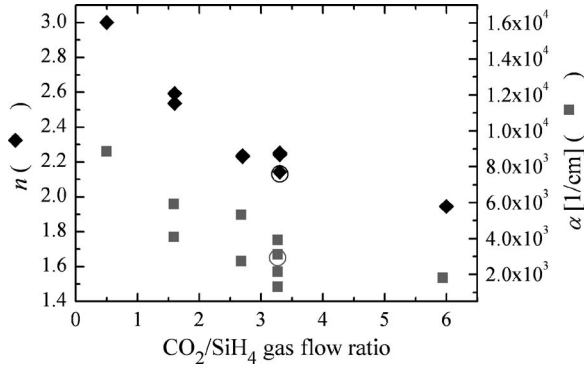


FIG. 1. Refractive index  $n$  and absorption coefficient  $\alpha$  at 600 nm of SiO-based layers estimated by fitting transmittance and reflectance spectra (full symbols) and ellipsometry measurements (empty circles).

24%, as shown in Fig. 2. Conversely, the conductivity is reduced by the same magnitude when increasing the  $\text{CO}_2/\text{SiH}_4$  from 1.6 to 3 with fixed  $\text{PH}_3/\text{SiH}_4$  ratio of 24%. Similar results have been previously observed for doped  $a\text{-SiO}_x\text{:H}$  layers.<sup>10</sup>

Figure 3 shows the EQE and absorbance of micromorph cells deposited in one deposition run with SOIR layers of different thicknesses. The difference in EQE due to the different SOIR thicknesses can be observed for wavelengths above 500 nm, as shorter wavelengths are absorbed in the top cell. The EQE of the top cell increases between 500 and 800 nm with increasing SOIR thickness, leading to a current gain in the  $a\text{-Si:H}$  cell of 1.0  $\text{mA}/\text{cm}^2$  for a 95-nm-thick SOIR. In the same spectral range, the EQE of the bottom cell decreases due to a reduced light intensity reaching the bottom cell, decreasing its current by 1.5  $\text{mA}/\text{cm}^2$ . Interference fringes can be observed in the sum of EQEs ( $\text{EQE}_{\text{top}} + \text{EQE}_{\text{bottom}}$ ) as well as in the absorbance of the device. With an optimized front ZnO layer and a SOIR thickness of 95 nm, a 1.2  $\text{cm}^2$  micromorph cell deposited entirely in the same reactor reaches an initial efficiency of 12.2% (Fig. 4). In comparison, the same cell without SOIR would have a  $J_{\text{sc}}$  of  $\sim 11 \text{ mA}/\text{cm}^2$  and an initial efficiency around 11.2%.

The main challenge for SOIR reflectors is to maintain a sufficiently high electrical conductivity while reducing as much as possible  $n$  and  $\alpha$  by incorporating oxygen into the Si films. The SOIR layers used in the micromorph devices have a low conductivity of  $10^{-9} \text{ S}/\text{cm}$  as measured on glass

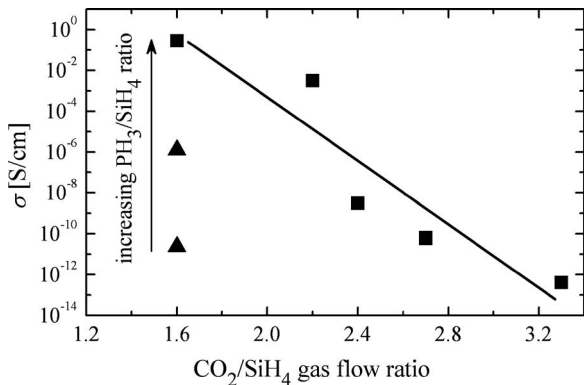


FIG. 2. In-plane dark conductivity  $\sigma$  at room temperature of SiO-based layers deposited on glass vs  $\text{CO}_2/\text{SiH}_4$  gas flow ratio.  $\text{PH}_3/\text{SiH}_4 = 0.024$  for (■) and 0.002 and 0.008 for (▲).

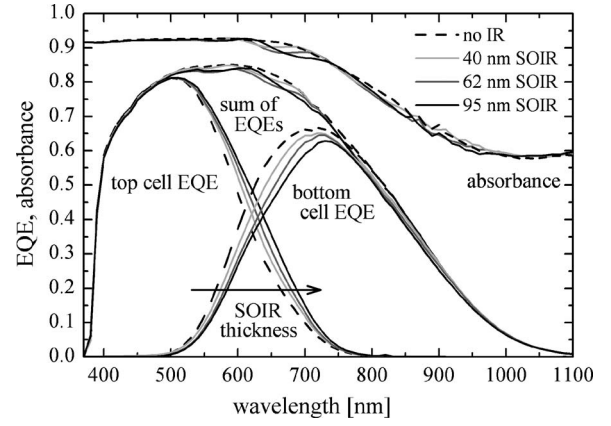


FIG. 3. EQE and absorbance of micromorph cells deposited in the KAI-S reactor without IRL (---) and with SOIR layers with different thicknesses (light gray=40 nm, and gray=62 nm, and black=95 nm).

in coplanar configuration, regardless of illumination. For layers with conductivities below  $10^{-5} \text{ S}/\text{cm}$ , we measure a silicon crystalline fraction between 2% and 10%. These values are too low to increase in-plane conductivity by percolation through doped Si nanocrystallites. However, the micromorph cells using the SOIR with low in-plane conductivity of  $10^{-9} \text{ S}/\text{cm}$  show only a moderate increase in series resistance of  $\sim 2 \Omega \text{ cm}^2$ , which is remarkably lower than the  $10^4 \Omega \text{ cm}^2$  that can be expected from the measured in-plane conductivity. This difference between the in-plane conductivity measured on glass and the perpendicular conductivity of the layer in the cell is likely due to the growth of microcrystalline Si grains, as detected in the Raman spectroscopy measurements, penetrating through the SiO-based layer. In the cell, their growth is enhanced from the beginning of the film by the underlying  $\mu\text{c-Si:H}$  doped layer, which allows the creation of high-conductivity passages across the SOIR. Hence we postulate the existence of a low conductivity amorphous SiO matrix, with a high transversal conductivity, i.e., conductivity approximately perpendicular to the substrate's plane, created by the crystalline Si phase. Conversely, the low in-plane conductivity of the SOIR with respect to ZnO IRL ( $\sigma_{\text{ZnO\_IRL}} = 2 \times 10^2 \text{ S}/\text{cm}$ ) is actually a desired property because it eliminates the need for an additional insulating laser scribe after the deposition of the IRL, facilitating therefore the serial interconnection.<sup>5</sup> In addition, possible shunts in the top or the bottom cell are laterally

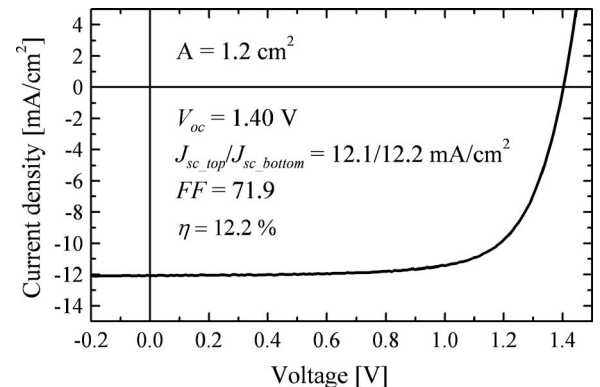


FIG. 4. Initial  $J$ - $V$  characteristics of a micromorph cell with 95 nm SOIR deposited in a small laboratory system.

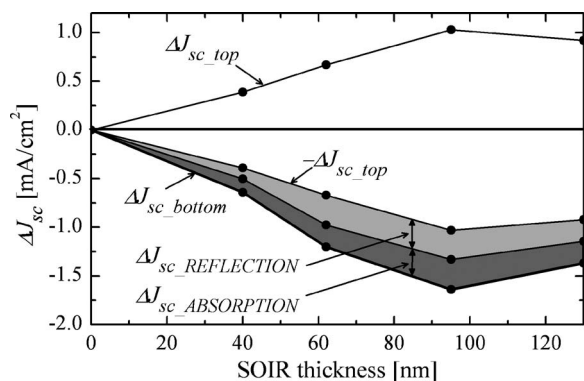


FIG. 5.  $\Delta J_{sc\_top}$  and  $\Delta J_{sc\_bottom}$  with different SOIR thicknesses. The gray surface between  $-\Delta J_{sc\_top}$  and  $\Delta J_{sc\_bottom}$  represents the total loss of current.

isolated and therefore do not drain current from large cell areas.

The presence of the intermediate reflector leads to a current gain in the top cell ( $\Delta J_{sc\_top}$ ) and to a current loss in the bottom cell ( $\Delta J_{sc\_bottom}$ ), as represented in Fig. 5. This transfer of current from the top to the bottom cell increases with the SOIR thickness up to  $\sim 100$  nm where it reaches a plateau.<sup>3</sup> The difference between  $-\Delta J_{sc\_top}$  and  $\Delta J_{sc\_bottom}$  represents the total loss of current in the whole device with respect to the cell without intermediate reflector. From the absorbance measurements shown in Fig. 3, we can calculate the current loss caused by the increased total reflectance with increasing SOIR thickness. We can therefore split the total loss of current in Fig. 5 into two parts: loss by increased reflectance and loss by optical absorption in the doped Si layers and the SOIR. The loss by absorption is mostly due to a thick *n*-doped Si layer that is used for this thickness series. For the best cell presented above, the doped layer thicknesses are decreased without significantly affecting  $V_{oc}$  or fill factor. By further tuning the properties of SOIR and device optimization, a reduction of all losses should be realizable and current gains as high as those reported for ZnO IRL should be achievable.

In summary, we have succeeded in fabricating and incorporating into micromorph devices SiO based layers with optical and electrical properties suitable to act as intermediate reflectors. The layers have a low refractive index between

2 and 2.4 at 600 nm and a low absorption as measured on glass. The layers are mixed phase and their conductivity perpendicular to the substrate is sufficiently high to permit unperturbed electrical functioning of the micromorph cell. The lateral conductivity is significantly lower than the conductivity of ZnO IRL, which reduces the negative impact of possible shunts and facilitates the series interconnection by laser scribing. The SOIR layers are produced in the same reactor as state of the art *p-i-n* solar cells, which eases the fabrication procedure and leverages the potential for cost reduction. So far, the best micromorph cells with incorporated SOIR entirely produced in the same reactor have an initial efficiency of 12.2%, which represents a relative increase of 8% over the same cell without IRL.

The authors gratefully acknowledge support by the Swiss Federal Energy Office (OFEN) under Grant No. 101191.

- <sup>1</sup>M. S. Bennett, J. L. Newton, and K. Rajan, *Proceedings of the Seventh European Photovoltaic Solar Energy Conference, Sevilla, Spain* (Reidel, Dordrecht, 1987), pp. 544–548.
- <sup>2</sup>D. Fischer, S. Dubail, J. A. Anna Selvan, N. Pellaton Vaucher, R. Platz, Ch. Hof, U. Kroll, J. Meier, P. Torres, H. Keppner, N. Wyrsh, M. Goetz, A. Shah, and K.-D. Ufert, *Proceedings of the 25th IEEE Photovoltaic Specialists Conference, Washington D. C., USA* (IEEE, New York, 1996), pp. 1053–1056.
- <sup>3</sup>D. Dominé, J. Bailat, J. Steinhäuser, A. Shah, C. Ballif, *Proceedings of the Fourth World Conference on Photovoltaic Energy Conversion, Hawaii, USA* (IEEE, New York, 2006), pp. 1465–1468.
- <sup>4</sup>S. Y. Myong, K. Sriprapha, S. Miyajima, and M. Konagai, *Appl. Phys. Lett.* **90**, 263509 (2007).
- <sup>5</sup>J. Meier, J. Spitznagel, S. Fay, C. Bucher, U. Graf, U. Kroll, S. Dubail, and A. Shah, *Proceedings of the 29th IEEE Photovoltaic Specialists Conference, New Orleans, USA* (IEEE, New York, 2002), pp. 1118–1121.
- <sup>6</sup>K. Yamamoto, A. Nakajima, M. Yoshimi, T. Sawada, S. Fukuda, T. Suezaki, M. Ichikawa, Y. Koi, M. Goto, T. Meguro, T. Matsuda, M. Kondo, T. Sasaki, and Y. Tawada, *Prog. Photovoltaics* **13**, 645 (2005).
- <sup>7</sup>A. C. W. Biebericher, A. R. Burgers, C. Devilee, and W. J. Soppe, in *Proceedings of 19th European Photovoltaic Solar Energy Conference, Paris, France* (WIP, Munich, 2004), pp. 1485–1488.
- <sup>8</sup>C. Droz, E. Vallat-Sauvain, J. Bailat, L. Feitknecht, and A. Shah, *Proceedings of 17th European Photovoltaic Solar Energy Conference, Munich, Germany* (WIP, Munich, 2002), pp. 2917–2920.
- <sup>9</sup>J. Meier, U. Kroll, E. Vallat-Sauvain, J. Spitznagel, U. Graf, and A. Shah, *Sol. Energy* **77**, 983 (2004).
- <sup>10</sup>A. Janotta, R. Janssen, M. Schmidt, T. Graf, and M. Stutzmann, *Phys. Rev. B* **69**, 115206 (2004).